SLIDING-MODE POSITION CONTROL OF A 1-DOF SET-UP BASED ON PNEUMATIC MUSCLES

J. Arenas, A. Pujana-Arrese, S. Riaño, A. Martinez-Esnaola and J. Landaluze

IKERLAN Technological Research Center
Control Engineering and Power Electronics Department
Arizmendiarrieta, 2. E-20500 Arrasate/Mondragon, Spain
E-mail: JArenas@ikerlan.es. Phone: +34-943712400

Abstract: A one-degree-of-freedom arm driven by pneumatic muscles has been designed and built in order to research the applicability of pneumatic artificial muscles in industrial applications. The experimental set-up is very non-linear and very difficult to control properly. As a reference, an enhanced PID controller was designed. At the same time, a sliding-mode controller based on an observer was designed and implemented. Firstly, this paper presents the experimental set-up and the system's linear models. After that, it focuses on the process of designing the sliding-mode controller. Finally, some results obtained in simulation as well as experimentally are presented.

Keywords: Pneumatic system, robot arm, sliding-mode control, PID control, robust control.

1. INTRODUCTION

The Ikerlan research centre is working on the design of an upper limb IAD (Intelligent Assist Device) (Martinez, *et al.*, 2007), a wearable exoskeleton oriented to help the user perform a routine activity in the workplace. One of the design specifications was to use, if possible, non-conventional actuators. Between the different alternatives, pneumatic artificial muscles – or McKibben muscles – are very interesting. For the purpose of researching their applicability in this kind of applications, an experimental one-DoF arm powered by pneumatic muscles manufactured by Festo was designed and constructed.

The experimental set-up resulted to be very non-linear and very difficult to control properly. Due to the fact that the results obtained with a classical PI controller were not good, robust control techniques were considered. For pneumatic muscles, the application of different control techniques is found in the literature, but a good performance requires the use of robust or non-linear control techniques (Thanh and Ahn, 2006; Balasubramanian and Rattan, 2005). Therefore, a non-linear robust control technique, sliding-mode, was applied to design a position controller. At the same time, and as a reference, a PID based controller was enhanced with linear and non-linear internal loops. Previously, the set-up was modelled in *Dymola/Modelica* and validated experimentally (Pujana-Arrese, *et al.*, 2007), and linear models obtained.

This paper focuses on the design of a sliding-mode position controller for the one-DoF arm. After describing briefly the experimental set-up, this paper goes on to explain the control objectives and the nominal linear models used in the controller design process. Then, the sliding-mode design procedure and the controller obtained are presented. The resulting chattering phenomenon and its compensation are shown as well. For purposes of comparison, the structure of the enhanced PID controller is also stated. Finally, the paper concludes by presenting some experimental and in-simulation results.

2. EXPERIMENTAL SET-UP

A real picture of the set-up constructed can be seen in Figure 1, where two *DMSP-20-200N* pneumatic muscles manufactured by Festo perform the role of the actuator. It consists of a robotic arm, with a displacement of around 60º and a maximum mass to be moved at the tip of 8 kg. The arm mass is 0.987 kg and, considering that the arm is in the horizontal

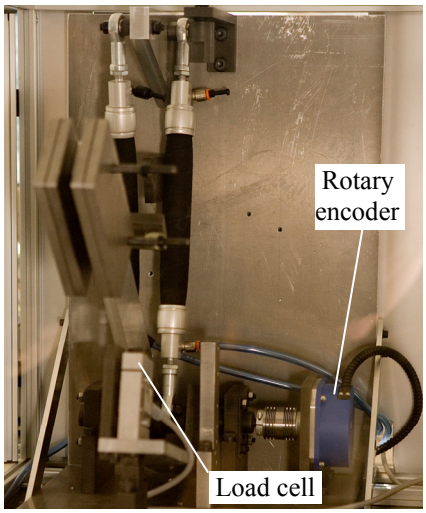

Fig. 1. Picture of the experimental set-up.

position, the centre of the arm mass with regard to the centre of rotation is at a height of 17.6 mm and at a horizontal distance of 205 mm. The additional masses are placed on the end of the arm at a horizontal length of 367 mm with regard to the centre of rotation. The set-up may be rotated so that the arm moves in a horizontal plane and the effects of gravity are therefore cancelled out.

A *Festo MPYE-5-1/8HF* pneumatic servovalve is used for actuation. The prototype includes a *FAGOR S-D90* encoder which supplies 180000 pulses per turn, and a load cell on the lower stop of the model. A more in detail description can be found in (Pujana-Arrese, *et al.*, 2007). Control algorithms were implemented in *Simulink* and code generated and downloaded in the control hardware by means of two of The MathWorks tools: *RTW* and *xPCTarget*.

3. SYSTEM MODELS

For the design of the robust controller the nominal conditions were considered to be when the robotic arm has a load of 3 kg at the tip, and that this load may be reduced, or increased up to 6 kg. The specifications therefore presume that the system must be robust for this load interval.

A full non-linear model of the prototype, experimentally validated, had previously been developed in *Dymola/Modelica* (Pujana-Arrese, *et al.*, 2007). On the basis of this model, reduced linear models for use in designing controllers were deduced. The nominal model is taken as being with a weight of 3 kg at the tip of the arm. Considering the system as a SISO system, where the input is the input voltage to the servovalve and the output is the angle position of the robotic arm, the resulting transfer function of the nominal model is as follows:

$$G_{3N}(s)=\frac{0.2s^2+31s+175}{0.075s^3+0.426s^2+9.36s+0.003}$$

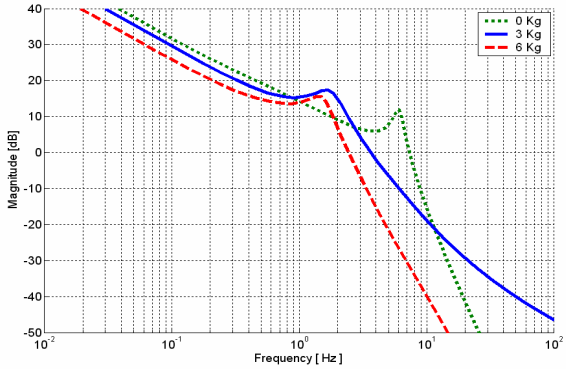

Fig. 2. Linear transfer functions for 0, 3 and 6 kg.

As extreme cases in the considered working range, it is contemplated a load of 6 kg at the tip of the arm, with the following reduced linear model:

$$G_6(s)=\frac{20.6s+63.5}{0.008s^4+0.09s^3+s^2+5.26s}$$

and the case of there being no weight on the arm, where the linear model is:

$$G_0(s)=\frac{0.33s^2+61.74s+142.5}{0.00003s^5+0.00153s^4+0.058s^3+1.96s^2+5.98s}$$

Figure 2 shows the plants in the frequency domain. As can be observed, the models show significant resonance. When the load is increased, the resonance frequency is reduced, together with the gain. The differences between the linear models are considered to be nominal model uncertainties. For purposes of obtaining these linear models, the effect of gravity has not been taken into account, as it was supposed that the arm moved in the horizontal plane. Also, these linear models do not reflect the significant influence of friction, which is very different throughout the robotic arm's range of displacement.

The application of the pneumatic muscles is intended for a human arm orthosis, where the set-point position is generated by the user's intention of movement, and it is not a path pre-set by a controller. On tuning the controller, small jumps in position, of 10º, have therefore been contemplated. The performance specifications are that the response to these jumps must be as quick as possible, with very little overshoot and no vibration.

4. CONTROLLER DESIGN

4.1 Brief review of sliding-mode theory considered

Sliding Mode Control (SMC) is a special case of Variable Structure Control (VSC). SMC techniques have been used in a diversity of systems due to their advantages as regards robustness in their application for control of non-linear systems. The design

methodology entails dividing the problem into two smaller-sized sub-problems: Firstly, establishing the sliding surface dynamics, which must be acceptable and may be linear, and then designing the surface that governs the system's behaviour when it is in sliding mode. A control law is subsequently designed, guaranteeing that the paths close to the sliding surface lead to that surface.

When the system is trapped on the surface, where the structure and the parameters have been established by the designer, the closed loop dynamics is totally determined by the equations that define it, and it is independent from any disturbance of the system parameters, thus achieving excellent robustness.

To develop the controller, development from Edwards and Spurgeon (1998) has been basically taken into account. A tracking requirement was incorporated using an integral action approach.

Initially, the following system is considered:

$$\begin{aligned} \dot{x}(t) &= Ax(t) + Bu(t) \\ y(t) &= Cx(t) \end{aligned} \tag{1}$$

which is assumed to be square, where A and B are the matrices representing the nominal system and $x(t)$ is the state vector. Considering an integral action, additional states $x_r \in \mathbb{R}^p$ are introduced:

$$\dot{x}_r(t) = r(t) - y(t) \tag{2}$$

where $r(t)$ represents the set-point value and $y(t)$ is the system output. Taking this into account, the new state vector is as follows:

$$\tilde{x} = \begin{bmatrix} x_1 \\ x_2 \end{bmatrix} \tag{3}$$

being $x_1 \in \mathbb{R}^n$ the old state vector and $x_2=x_r$ represents the additional states. In this way, the increased nominal system can be rewritten as follows:

$$\begin{aligned} \dot{x}_1(t) &= \tilde{A}_{11}x_1(t) + \tilde{A}_{12}x_2(t) + r(t) \\ \dot{x}_2(t) &= \tilde{A}_{21}x_1(t) + \tilde{A}_{22}x_2(t) + Bu(t) \end{aligned} \tag{4}$$

$$\begin{bmatrix} \tilde{A}_{11} & \tilde{A}_{12} \\ \tilde{A}_{21} & \tilde{A}_{22} \end{bmatrix} = \begin{bmatrix} 0 & -C_1 & -C_2 \\ 0 & A_{11} & A_{12} \\ 0 & A_{21} & A_{22} \end{bmatrix} \tag{5}$$

As previously explained, the sliding-mode control is based on taking the system to a surface where the closed loop dynamics will be governed by the equations established, free of any unmodelled disturbances. In this way, bearing in mind that a tracking requirement has been incorporated, the sliding surface is defined by:

$$\begin{aligned} S &= \left\{ \tilde{x} \in \mathbb{R}^{n+p} : S\tilde{x} = S_r r \right\} \\ S &= \begin{bmatrix} S_1 & S_2 \end{bmatrix} \end{aligned} \tag{6}$$

where S and S_r are design parameters governing the movement dynamics. S_1 will be of dimension n, and S_2 of dimension p. It can be deduced from (4) that the ideal sliding movement is given by:

$$\dot{x}_1(t) = (\tilde{A}_{11} - \tilde{A}_{12}M)x_1(t) + (\tilde{A}_{12}S_2^{-1}S_r + I)r(t) \tag{7}$$

where $M = S_2^{-1}S_1$. S must therefore be defined to set the system dynamics on the sliding movement. To establish the sliding surface S the system's uncertainties must be taken into account, estimated through the nominal models presented; to do this, a robust eigenstructure assignment was made, which sets the actual values of the closed loop system by design, thus defining the sliding surface S.

Once S has been set, the control signal for designing a sliding-mode controller including an integral action approach and a tracking requirement is:

$$u = u_L(\tilde{x}, r) + u_N \tag{8}$$

where the linear component is:

$$u_L(\tilde{x}, r) = L\tilde{x} + L_r r + L_{\dot{r}}\dot{r} \tag{9}$$

$$\begin{aligned} L &= -\left[SB\right]^{-1}(S\tilde{A} - \phi S) \\ L_r &= -\left[SB\right]^{-1}(\phi S_r + S_2 M) \\ L_{\dot{r}} &= \left[SB\right]^{-1} S_r \end{aligned} \tag{10}$$

and where S_r and ϕ are design matrices.

The non-linear component of the control law (8) will be a function of the surface S, multiplied by a gain K established in the design process. In classical sliding-mode a sign function is used:

$$u_N = -K \cdot \mathrm{sgn}(S\tilde{x}) \tag{11}$$

4.2 Observer design

The design of the controller described above must be able to measure the state vector. However, this is not possible in the physical system being studied, and an observer therefore needed to be designed in order to estimate it. To do this, the approach followed by

Walcott and Zak (1987) is used, such as it is cited in Edwards and Spurgeon (1998).

In a linear system such as (1), the observer can be expressed by the formula:

$$\dot{\hat{x}}(t) = A\hat{x}(t) + Bu(t) - G(C\hat{x}(t) - y(t)) + FB\nu \quad (12)$$

where $\hat{x}$ represents the state vector estimated. In this way, the observer takes the form of a system model, which is impelled by the misalignment between the plant output and the observer output. The linear gain G is calculated as follows:

$$G = T_0^{-1}\begin{bmatrix} A_{12} \\ A_{22} - A_{22}^{s} \end{bmatrix} \quad (13)$$

where T_0 is the matrix representing the change of coordinates between the given system and its canonical form and A_{22}^{s} is a diagonal matrix established in the design. ν is the sign function of $C\hat{x}(t) - y(t)$ multiplied by a design constant K. The matrix F is calculated by means of $F = B^{T}P$, where P is the solution to the Lyapunov equation:

$$A_{22}^{s}P + PA_{22}^{s\,T} + I = 0 \quad (14)$$

4.3 Controller implementation

On the basis of the nominal model G_{3N} the first step is to convert the system given by a transfer function into its expression by means of the state space, obtaining the A, B and C matrices required for the design (see Appendix). Once these matrices defining the system have been obtained, the next step is to design the observer to obtain the matrices G and F. To do this, the value A_{22}^{s} needs to be established. This was done by trial and error, setting the desired output estimation error pole.

After designing the observer, it was proceeded to design the sliding-mode controller in accordance with the equations described in the previous sections. The desired λ poles had to be set for the closed loop system, which provides the system robustness. The rest of the design matrices (see Appendix) were set experimentally to obtain good response performance.

4.4 Chattering compensation

In classical sliding-mode the equation (11) leads to undesirable phenomenon of oscillations, which is known as "chattering". It is a harmful phenomenon because it causes high controller activity and high heat losses in mechanical parts and power circuits. Several strategies for significantly reducing this phenomenon can be found in the literature: Perruquetti and Barbot (2002) saturate the changing speed of the sign function so that the non-linear component of the control does not change sign in an sample time; another possibility, described by Utkin, *et al.* (1999), is to replace the sign function by another function which remains invariable once the sliding within a band has been guaranteed, for example s/ϕ, where ϕ is the boundary layer thickness; and a third alternative, very widely used, consists of replacing the sign function by the tanh function. The first of these methods has been used for the case in hand.

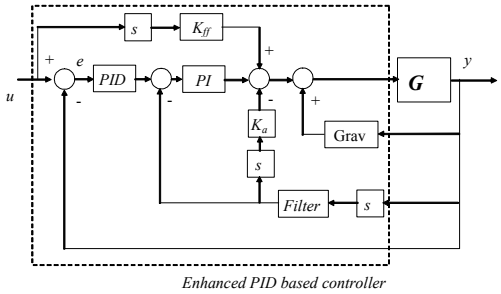

Fig. 3. Structure of the enhanced PID based control.

4.5 Enhanced PID based controller

Initially, a classic PI controller was adjusted so that it served as a reference for comparing the results obtained with other, more advanced, controllers. On the basis of this basic controller, the structure was completed with other internal linear and non-linear loops. Figure 3 shows the structure of the most elaborate controller constructed. The position PID was complemented with a speed loop and an acceleration loop. A speed feedforward was also added to improve the dynamic response. A more internal non-linear loop partly compensated the effects of gravity. For the basic PI controller the gains were adjusted to the values K_p=0.062 and K_i=0.029. For the case of the enhanced PID the tuned gains were K_p=8.5, K_i=0.009, K_d=0.8, K_{vp}=0.02, K_{vi}=0.005, K_{ff}=0.0025 and K_a=0.0002.

5. RESULTS

5.1 Results in simulation

The sliding-mode controller designed was previously tested in simulation. As an example of the tuning performed, Figure 4 shows the response of the linear system simulated to a 10º/s ramp, varying the set-point position from 40º to 50º, the angle being measured with respect to the vertical. The results shown are those obtained in three cases: with the nominal model of 3 kg at the tip, with a load of 6 kg

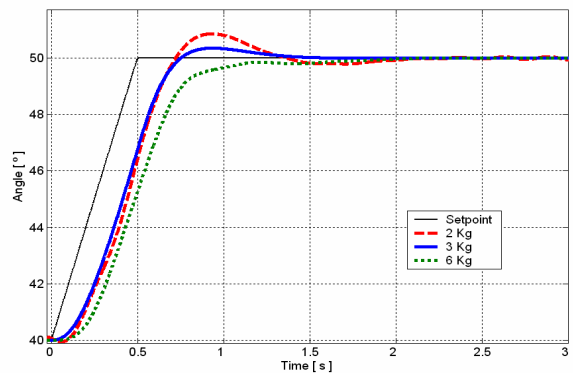

Fig. 4. Results in simulation.

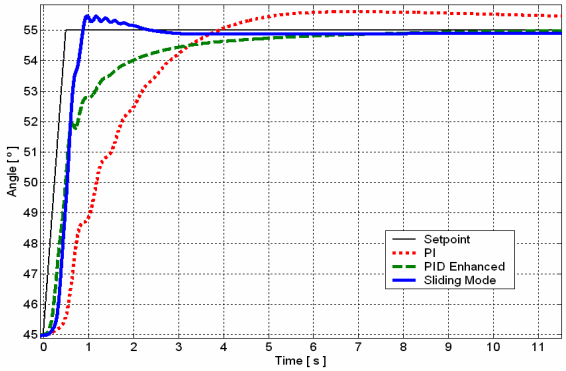

Fig. 6. Experimental results in lower zone.

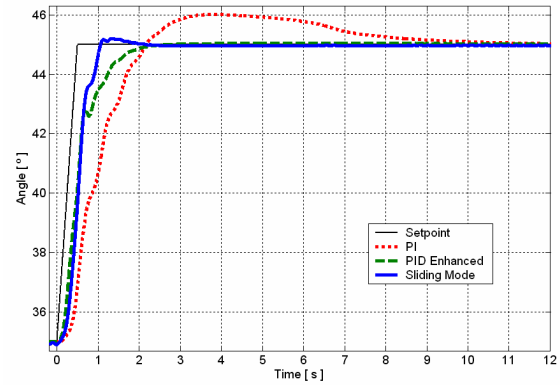

Fig. 5. Experimental results in the middle of zone.

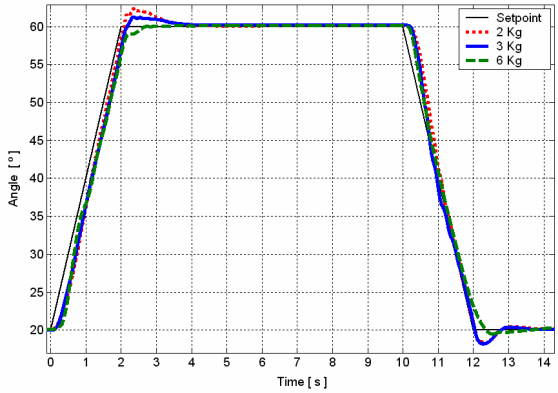

Fig. 7. Experimental results with different tip masses.

at the tip, and with 2 kg. The system response with 2 and 3 kg shows a lesser upward slope time, although it finally exceeds the set-point value. When this overshoot is compensated for, the error rapidly decreases until it reaches zero. With 6 kg, the system does not show any overshoot but the establishment time is longer. It could be underlined the fact that the system shows no vibration when the nominal load is increased by 100%, thus proving the robustness of the sliding-mode controller. When the load is decreased the performance is a bit worse.

5.2 Experimental results

Both the sliding-mode controller and the enhanced PID presented were discretized with a sample time of 2 ms. As in the PID controller, also for the sliding-mode controller an internal loop was added which partly compensated the effects of gravity. Due to the significant effect of the non-linearities on the movement of the prototype throughout its entire range, the results for two different areas are shown, comparing the responses obtained with the sliding-mode controller to the responses for the PI and the enhanced PID. Figure 5, which corresponds to a jump in the intermediate area of the displacement range, shows the experimental results obtained with the weight considered as nominal, 3 kg. It can be seen that for the PI control response both the overshoot and establishment time are excessive, while the response of the enhanced PID is suitably in accordance with the set-point value until a vibration occurs which changes its dynamics and worsens the establishment time. The sliding-mode controller, with slight vibration in the overshoot area, is also very fast, and cancels out the stationary error.

Figure 6 shows the system's response in the same conditions as above, but in the area showing worse performance: it corresponds to a jump at the end of the displacement range, when the arm moves into quasi-horizontal position. Again, the PI control shows a response with considerable overshoot and establishment time, in addition to vibration. On the other hand, it can be observed how the response of the improved PID substantially increases its establishment time with respect to the previous zone. The sliding-mode controller reaches the set-point position in less than one second, although the vibration in the overshoot area is increased with respect to that occurring in the previous jump.

To corroborate the robustness of the sliding-mode controller, Figure 7 shows the response of the arm with a load of 2, 3 and 6 kg to a set-point position change of 40º (the 0º reference corresponds to the vertical position). In all the cases, the responses show good establishment times, although, as anticipated on simulation and as a result of the tuning performed, overshoot occurred in the test carried out with 2 and 3 kg. In any case, the robustness of the sliding-mode control is evident, as the differences between the responses are very slight.

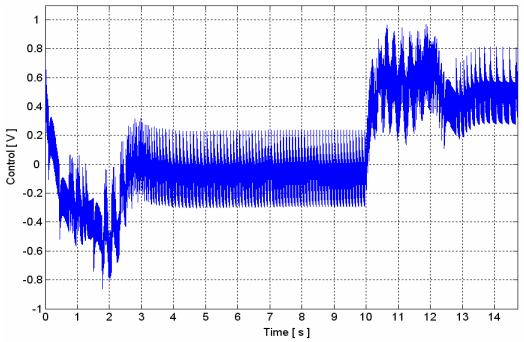

Fig. 8. Chattering effect in the control signal.

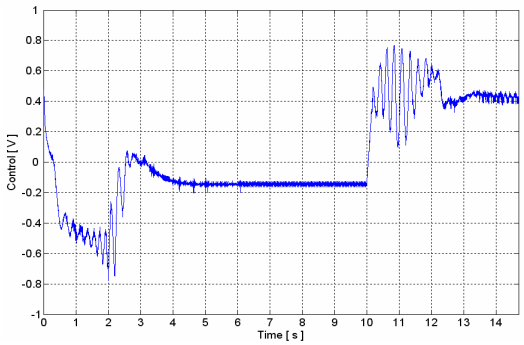

Fig. 9. Control signal with anti-chattering algorithm.

As mentioned in section 4.4, the chattering phenomenon must be taken into account in the design of the sliding-mode controller, attempting to reduce it. With this object in mind, the saturation to the non-linear control component was implemented, limiting the speed at which it can change the sign function to 10º/s. Figure 8 shows the control signal for the test shown in Figure 7 in the case of 3 kg, with no anti-chattering strategy being used. Much high-frequency activity can be observed. Figure 9 shows the control signal for the same case, but using the anti-chattering strategy described. The system's response in both cases is totally identical, with no loss of performance.

6. CONCLUSIONS

This paper presents the design of a sliding-mode position controller for an experimental one-DoF prototype based on pneumatic muscles. The prototype is very non-linear according to the displacement zones, and very difficult to control with a classical PI type controller. Observer-based design was used for the sliding-mode position control, and the controller obtained proved to be robust as regards performance. Also, as a reference for comparing the results, an improved PID controller with linear and non-linear loops was considered. The data presented show the superiority of the sliding-mode controller.

ACKNOWLEDGMENT

The material used in this paper was partly supported by the Spanish Ministry of Education and Science and European FEDER Fund (research project DPI2006-14928-C02-01).

REFERENCES

Balasubramanian, K. and K.S. Rattan (2005). Trajectory tracking control of a pneumatic muscle system using fuzzy logic. *NAFIP'2005, Annual Meeting of the North American Fuzzy Information Precessing Society.*

Martinez, F., I. Retolaza, E. Lecue, J. Basurko and J. Landaluze (2007). Preliminary design of an upper limb IAD (Intelligent Assist Device). *9th European Conference for the Advancement of Assistive Technology, AAATE 2007, October 3rd-5th, Donostia.*

Pujana-Arrese, A., J. Arenas, L. Maruri, A. Martinez-Esnaola and J. Landaluze (2007). Modelling and Validation of a 1-DOF Arm Powered by Pneumatic Muscles. *Industrial Simulation Conference ISC'2007. 11-13 June, Delft, Holland.*

Thanh, T.D.C., and K.K. Ahn (2006). Nonlinear PID control to improve the control performance of 2 axes pneumatic artificial muscle manipulator using neural network. *Mechatronics*, **no. 16**, pp. 577-587.

Edward, C. and S.K. Spurgeon (1998). *Sliding Mode Control. Theory and Applications*. Taylor & Francis Ltd. ISBN 0-7484-0601-8.

Perruquetti, W. and J.P. Barbot (2002). *Sliding Mode Control in Engineering*. Marcel Dekker, Inc. ISBN 0-8247-0671-4.

Utkin, V., J. Guldner and J. Shi, J (1999). *Sliding Mode Control in Electromechanical Systems*. Taylor & Francis. ISBN 0-7484-0116-4.

Walcott, B.L. and S.H. Zak (1987). State observation of nonlinear uncertain dynamical systems. *IEEE Transaction on Automatic Control,* **no.32**, pp.166-170.

APPENDIX

The design values used in equations (1), (6), (9), (10) and (12) are as follows:

$$A = \begin{bmatrix} -5.7176 & -125.6904 & -0.0044 \\ 1 & 0 & 0 \\ 0 & 1 & 0 \end{bmatrix} ; \; B = \begin{bmatrix} 1 \\ 0 \\ 0 \end{bmatrix}$$

$$C = \begin{bmatrix} 2.9 & 415.3 & 2350 \end{bmatrix}$$

$$S = \begin{bmatrix} 0 & -1 & -9.28 & -33.64 \end{bmatrix}$$

$$L = \begin{bmatrix} 0 & -23.5624 & 93.5496 & -672.7956 \end{bmatrix}$$

$$L_r = 0.2863 \; ; \; L_i = 0.0143$$

$$S_r = -0.0143 \; ; \; P = 0.025$$

$$\phi = -0.2 \; ; \; K = 0.02$$

$$G = \begin{bmatrix} -1.9609 \\ 0.3491 \\ 0 \end{bmatrix}$$

$$F = 14.3243$$

$$K \text{ (obs)} = -2$$